Biophysical Journal, Volume *114*

Supplemental Information

Motor Reattachment Kinetics Play a Dominant Role in Multimotor-Driven Cargo Transport

Qingzhou Feng, Keith J. Mickolajczyk, Geng-Yuan Chen, and William O. Hancock

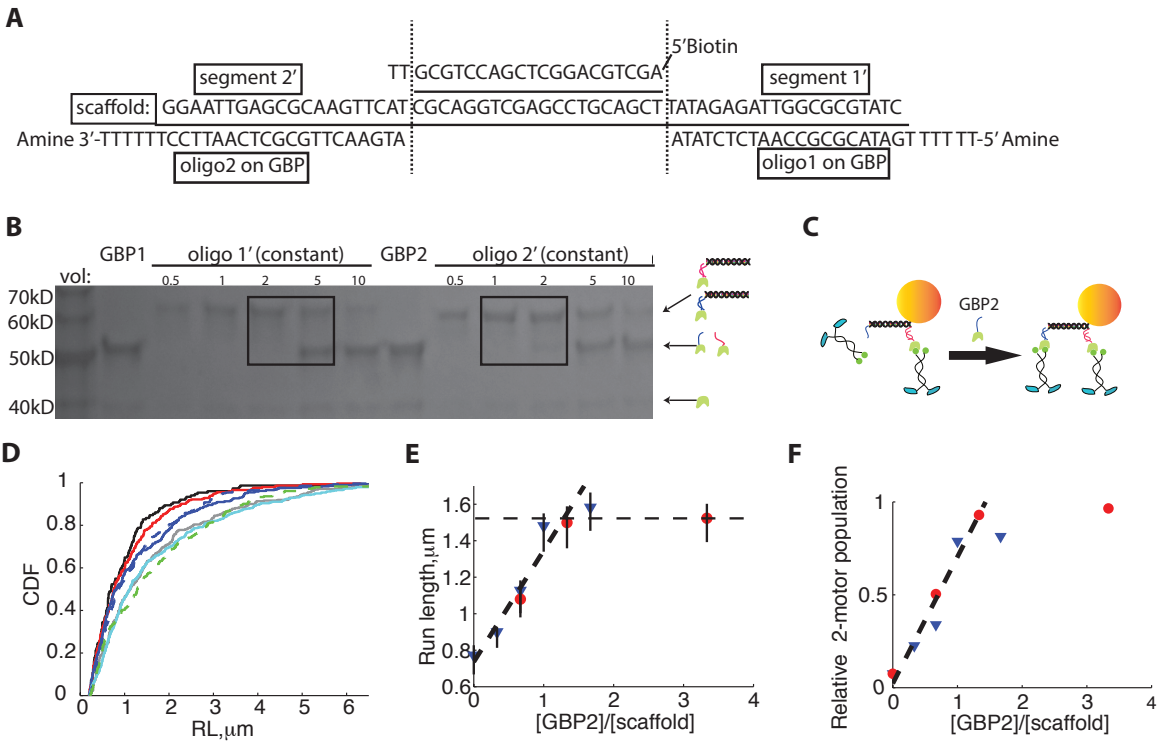

Figure S1: Characterization and quantification of motor-scaffold assemblies (related to Fig. 1)
(A) Diagram of sequences used for DNA scaffold design. Middle sequence is scaffold ssDNA; oligo1 and oligo2 on bottom are ssDNA linked to the GBP to make GBP1 and GBP2; and biotin-labeled ssDNA on top is labeled with a streptavidin-coated quantum dot for imaging.
(B) Quantification of oligo-GBP concentration by SDS-PAGE. A constant volume of 5 μM complementary oligo (1′ or 2′) was mixed with increasing volumes of GBP1 or GBP2 (GBP volume relative to oligo volume labeled for each lane). At substoichiometric GBP1 or GBP2 levels, only the upper band, corresponding to fully hybridized GBP1-1′ and GBP2-2′ was observed (see diagram at right), but when the [GBP] exceeded the complementary oligo (1′ or 2′) concentration, a lower band corresponding to unhybridized GBP was observed. Thus, the upper and lower limits for the concentration of GBP1 and GBP2 were measured by the switching points (box in the gel), and for GBP1 were [1μM, 2.5μM] and GBP2 [2.5μM, 5μM], respectively.
(C) Configuration of experiments. DNA scaffolds were mixed with 2-fold excess GBP1 and 10-fold excess motors to generate one-motor scaffold assemblies. To generate two-motor assemblies, increasing concentrations of GBP2 were added until all scaffolds are saturated with two motors.
(D) Cumulative distribution of run lengths for scaffolds with one kinesin-1 bound through GBP1, mixed with varying concentrations of GBP2 to achieve two-motor assemblies. Solid lines: 12 nM scaffold with 0 nM (black), 4 nM (red), 8 nM (blue), 12 nM (gray), and 20 nM (cyan) GBP2. Dashed lines: 6 nM scaffold with 4 nM (blue), 8 nM (purple), and 20 nM (green) GBP2. The one- and two-motor kinesin-1 run lengths in **Figure 1C** correspond to the 0 nM GBP2 (solid black) and 20 nM GBP2 (dashed green) traces.
(E) Mean run length (from panel D) as a function of the GBP2/scaffold ratio. As the ratio of GBP2 to scaffold increases, the population shifts from one-motor to two-motor run lengths. Red circles represent 12 nM scaffold data, while blue triangles represent 6 nM scaffold data. Dashed lines denote linear increase in run length with increasing two-motor populations and plateau when all scaffolds contain two motors.
(F) Bi-exponential fits to run length distributions as an alternate method to confirm full occupancy of two-motor complexes. Run length distributions in (D) were fit to the equation: $RL = 1 - C_{1\_motor}e^{-\frac{RL}{RL_1}} - C_{2\_motor}e^{-\frac{RL}{RL_2}}$; where RL_1 and RL_2 are the one- and two-motor run lengths, and C_1 and C_2 are the relative concentrations of one- and two-motor assemblies from the fits. Fraction two-motor population, $C_2/(C_1 + C_2)$, is plotted as a function of the GPB2/scaffold ratio, with red circles denoting 12 nM scaffold data and blue triangles denoting 6 nM scaffold data.

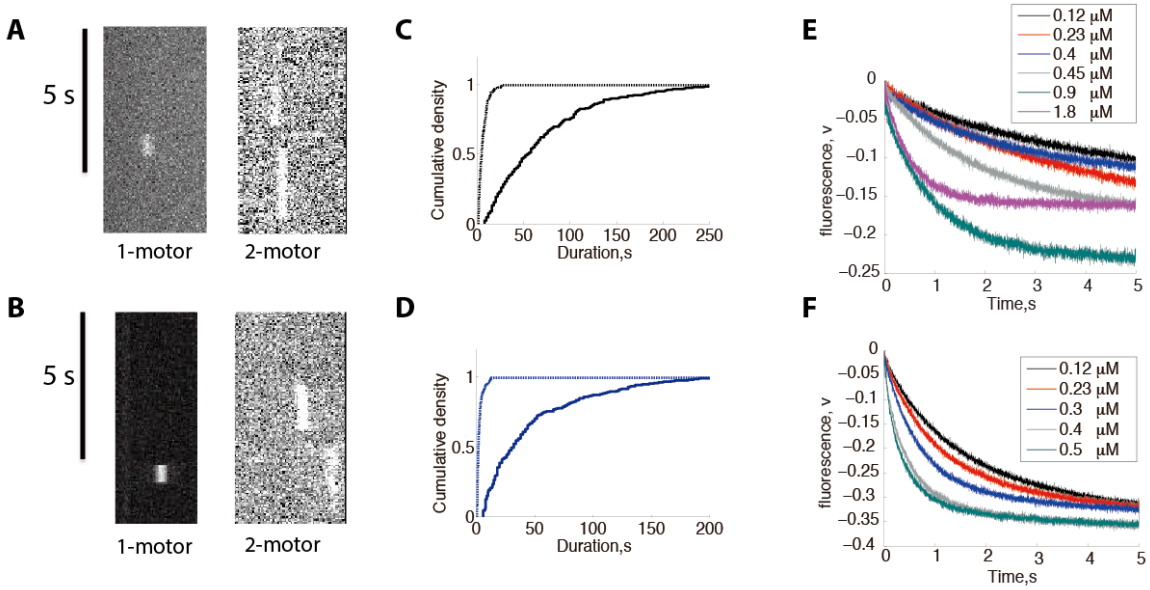

Figure S2: Analysis of $k_{reattach}$ at 10 µM ATP and raw data for bimolecular on-rate experiments (related to Fig. 2)

(A and B) Kymographs of one-motor (left) and two-motor (right) binding durations in 3mM ADP for kinesin-1 (A) and kinesin-2 (B).

(C and D) CDF of one-motor (dashed line) and two–motor (solid line) binding durations in 10 µM ADP for kinesin-1 (C) and kinesin-2 (D).

(E and F) Fluorescence traces from stopped-flow for mantADP release from kinesin-1 (E) and kinesin-2 (F) motors following fast mixing with varying concentration of microtubules. Motors incubated with mantADP were flushed against microtubules containing 3 mM unlabeled ADP to prevent mantADP rebinding, and the observed off-rate of mantADP was measured by fitting single exponentials to the fluorescence decay traces.

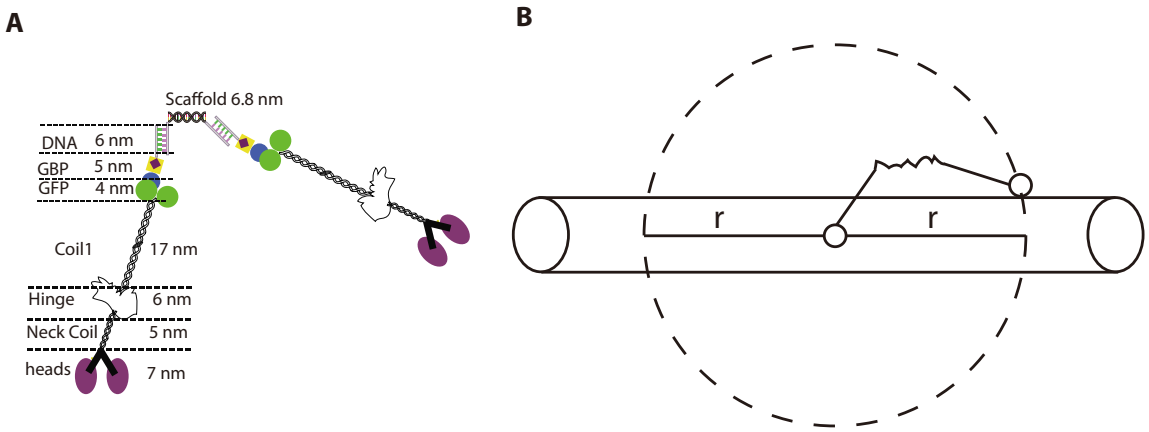

Figure S3: Effective tubulin concentration estimation (related to Fig. 2)
(A) To-scale diagram of the motor-scaffold complex. Component names are shown in the left and estimated sizes of each component are shown on the right, estimated as follows. The neck-coil and coil-1 consist of 35 and 112 residues, respectively. The hinge consists of 55 amino acids and is modeled as a worm-like chain with contour length 20 nm, persistence length 2 nm, and mean end-to-end distance =sqrt(l_p*l_c). Oligo connecting GBP to scaffold is 20 bases and the scaffold is also 20 bp. Note that coiled-coil and tail domains of the two motors are identical.
(B) Calculation of effective local tubulin concentration for a tethered motor. Effective concentration was calculated by estimating the number of tubulin subunits accessible in the search volume of the tethered motor. The end-to-end distance between the two motors is approximately 100 nm (**Fig. S3A**). If the tethered motor searches a hemispheric volume above the microtubule, that volume is 2.0 x 10^{-18} L. For a 200-nm length of microtubule in which the top six protofilaments are exposed, there are 150 tubulin subunits (8 nm per tubulin), corresponding to 125 μM tubulin. Note that this calculation assumes that the tether connecting the two motors is zero stiffness up to its contour length. Notably, including a restoring force or considering a shorter tether actually leads to a higher estimated local concentration because volume scales with r^3 while the number of tubulin subunits scales with r.

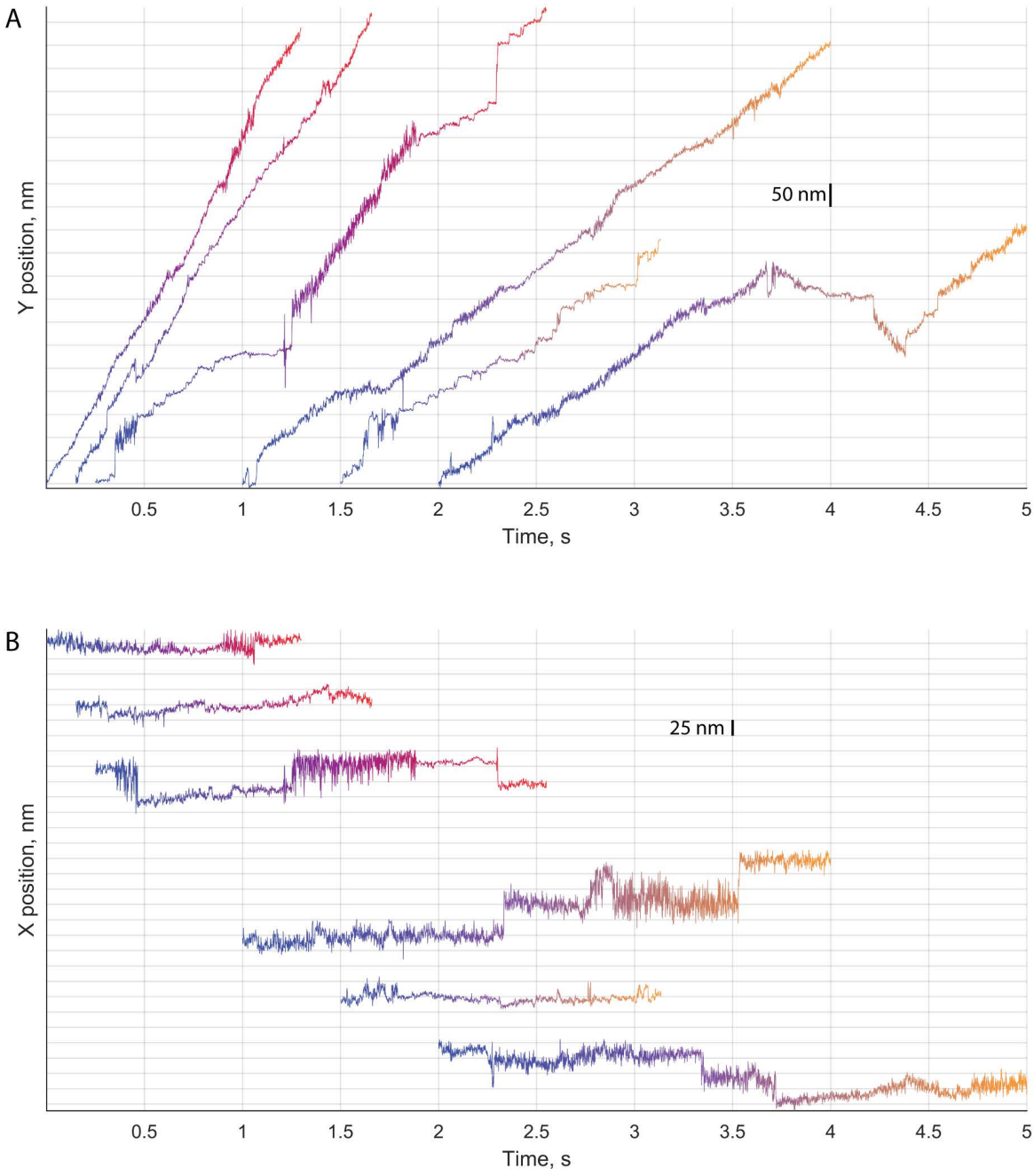

Figure S4: High-resolution gold nanoparticle tracking data as a function of time (related to Fig. 3)
Example traces shown in **Fig. 3** are replotted as Y, position along the microtubule (A) and as X, position perpendicular to the microtubule (B) versus time. Kinesin-1 pairs are shown in blue-red, and kinesin-2 pairs are shown in blue-yellow. Lower X values represent movements to the right of the microtubule. Color coding per data point matches the color coding in **Fig. 3**. All data were acquired at 1,000 frames per second.

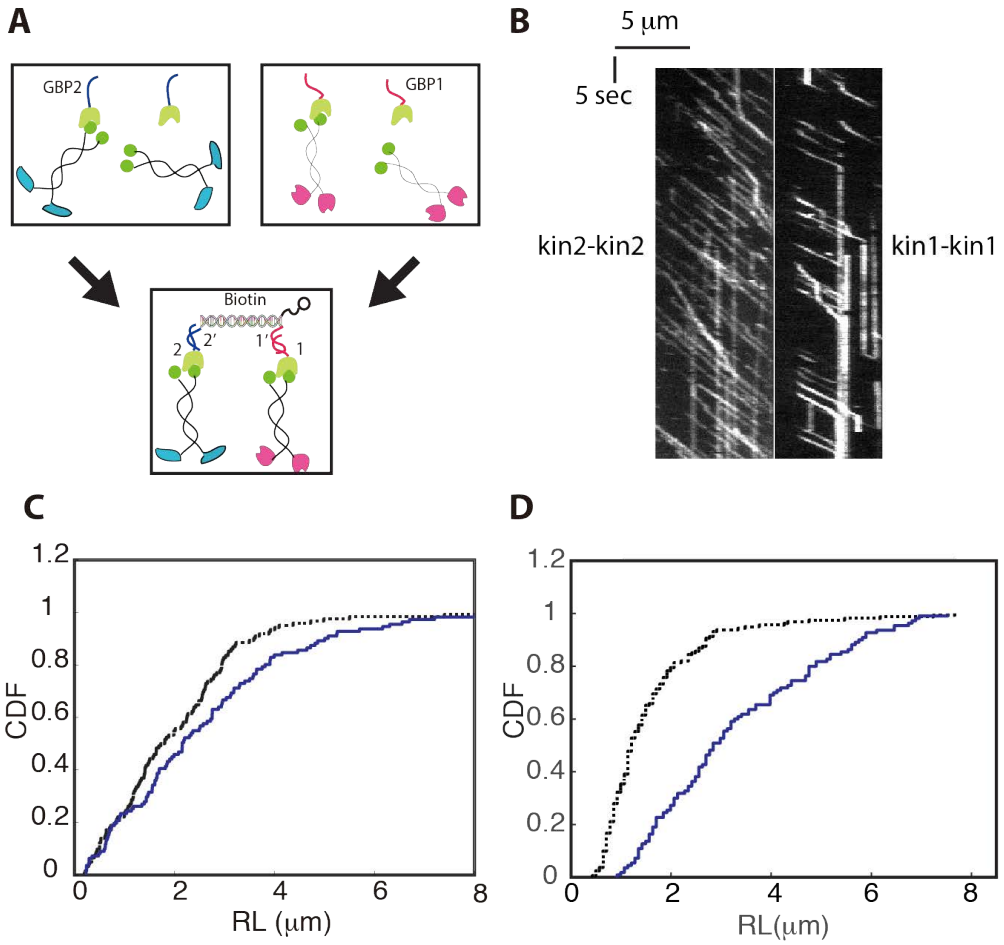

Figure S5: Run lengths of Kin1-Kin2 pairs and run lengths in the presence of roadblocks (related to Fig. 4)
(A) Procedure for making Kin1-Kin2 pairs (related to **Fig. 4A and B**). Kinesin-1 was mixed with GBP2, kinesin-2 was mixed with GBP1, and then scaffolds were added. The procedure used excess motors to GBP to ensure that all GBP had motors bound, and used excess GBP to scaffold to ensure that all scaffold sites were occupied with motors. Scaffold fluorescence was visualized, avoiding problems of any excess motors in the system.
(B) Kymograph of Kin2-Kin2 pairs (left) and Kin1-Kin1 pairs (right) with 2.65% roadblocks (related to **Fig. 4C**).
(C) CDF of Kin1-Kin1 (black dashed line) and Kin2-Kin2 (blue line) run lengths in the absence of roadblocks (related to **Fig. 4C**).
(D) CDF of Kin1-Kin1 (black dashed line) and Kin2-Kin2 (blue line) run lengths in the presence of 2.65%roadblocks (related to **Fig. 4C**).

Table S1: Microtubule binding durations under different nucleotide conditions.

	Run length in 3 mM ATP		
	1 motor	2 motor	Fold enhancement
Kinesin-1	0.77±0.16 μm	1.62±0.23 μm	2.1
Kinesin-2	0.65±0.13 μm	2.38±0.26 μm	3.7
Kin1-Kin2		2.2±0.39 μm	
	Run Length after correction [a]		
	1 motor	2 motor	Fold enhancement
Kinesin-1	0.80 μm	2.1 μm	2.6
Kinesin-2	0.65 μm	3.6 μm	5.5
Kin1-Kin2		3.2 μm	
	Binding duration in 3mM ADP		
	T_1	T_2	$k_{reattach}$
Kinesin-1	0.72±0.15 s	1.86±0.31 s	4.4±1.8 s^{-1}
Kinesin-2	0.50±0.11 s	2.51±0.39 s	16.1±6.6 s^{-1}
	Binding duration in 10 μM ADP		
	T_1	T_2	$k_{reattach}$
Kinesin-1	5.1±2.0 s	64.1±8.9 s	4.6±3.2 s^{-1}
Kinesin-2	2.1±0.5 s	42.9±8.9 s	18.7±8.0 s^{-1}

[a] Run length data after correcting for the effect of finite microtubule lengths on measured run lengths (see Methods for details).